

Laser absorption spectroscopy for high temperature H_2O time-history measurement at 2.55 μm during oxidation of hydrogen

Yu-Dan Gou(苟于单), De-Xiang Zhang(张德翔), Yi-Jun Wang(王易君), Chang-Hua Zhang(张昌华), Ping Li(李萍), Xiang-Yuan Li(李象远)

Citation: Chin. Phys. B . 2018, 27(7): 074213. **doi:** 10.1088/1674-1056/27/7/074213

Journal homepage: http://cpb.iphy.ac.cn; http://iopscience.iop.org/cpb

What follows is a list of articles you may be interested in

Analysis of algebraic reconstruction technique for accurate imaging of gas temperature and concentration based on tunable diode laser absorption spectroscopy

Hui-Hui Xia(夏晖晖), Rui-Feng Kan(阚瑞峰), Jian-Guo Liu(刘建国), Zhen-Yu Xu(许振宇), Ya-Bai He(何亚柏)
Chin. Phys. B . 2016, 25(6): 064205. **doi:** 10.1088/1674-1056/25/6/064205

Lasing dynamics study by femtosecond time-resolved fluorescence non-collinear optical parametric amplification spectroscopy

Wei Dang(党伟), Qing Liao(廖清), Peng-Cheng Mao(毛鹏程), Hong-Bing Fu(付红兵), Yu-Xiang Weng(翁羽翔)
Chin. Phys. B . 2016, 25(5): 054207. **doi:** 10.1088/1674-1056/25/5/054207

Wavelength modulation spectroscopy at 1530.32 nm for measurements of acetylene based on Fabry-Perot tunable filter

Yun-Long Li(李运龙), Bing-Chu Yang(杨兵初), Xue-Mei Xu(许雪梅)
Chin. Phys. B . 2016, 25(2): 024208. **doi:** 10.1088/1674-1056/25/2/024208

Sensitive absorption measurements of hydrogen sulfide at 1.578 μm using wavelength modulation spectroscopy

Xia Hua, Dong Feng-Zhong, Wu Bian, Zhang Zhi-Rong, Pang Tao, Sun Peng-Shuai, Cui Xiao-Juan, Han Luo, Wang Yu
Chin. Phys. B . 2015, 24(3): 034204. **doi:** 10.1088/1674-1056/24/3/034204

Dynamic thermal modeling and parameter identification for monolithic laser diode module

Li Jin-Yi, Du Zhen-Hui, Ma Yi-Wen, Xu Ke-Xin
Chin. Phys. B . 2013, 22(3): 034203. **doi:** 10.1088/1674-1056/22/3/034203

Laser absorption spectroscopy for high temperature H_2O time-history measurement at 2.55 μm during oxidation of hydrogen*

Yu-Dan Gou(苟于单)[1], De-Xiang Zhang(张德翔)[1], Yi-Jun Wang(王易君)[1], Chang-Hua Zhang(张昌华)[1,†], Ping Li(李萍)[1], and Xiang-Yuan Li(李象远)[2]

[1] *Institute of Atomic and Molecular Physics, Sichuan University, Chengdu* 610065, *China*
[2] *College of Chemical Engineering, Sichuan University, Chengdu* 610065, *China*

(Received 30 January 2018; revised manuscript received 15 March 2018; published online 25 June 2018)

Concentration time-histories of H_2O were measured behind reflected shock waves during hydrogen combustion. Experiments were conducted at temperatures of 1117–1282 K, the equivalence ratios of 0.5 and 0.25, and a pressure at 2 atm using a mixture of H_2/O_2 highly diluted with argon. H_2O was monitored using tunable mid-infrared diode laser absorption at 2.55 μm (3920.09 cm^{-1}). These time-histories provide kinetic targets to test and refine reaction mechanisms for hydrogen. Comparisons were made with the predictions of four detailed kinetic mechanisms published in the last four years. Such comparisons of H_2O concentration profiles indicate that the AramcoMech 2.0 mechanism yields the best agreement with the experimental data, while CRECK, San Diego, and HP-Mech mechanisms show significantly poor predictions. Reaction pathway analysis for hydrogen oxidation indicates that the reaction $H+OH+M=H_2O+M$ is the key reaction for controlling the H_2O formation by hydrogen oxidation. It is inferred that the discrepancy of the conversion percentage from H to H_2O among these four mechanisms induces the difference of performance on H_2O time-history predictions. This work demonstrates the potential of time-history measurement for validation of large reaction mechanisms.

Keywords: tunable diode laser absorption spectroscopy, H_2O time-history profile, combustion process, reaction mechanism

PACS: 42.62.Fi, 42.55.Px, 82.33.Vx **DOI:** 10.1088/1674-1056/27/7/074213

1. Introduction

Growing concerns about the environmental problems and the shortage of energy resources have led to seeking clean-alternative fuels to deal with environmental pollution and energy security. Hydrogen is a promising alternative due to its advantageous combustion characteristics, such as high flame speed and broad burn limit, which are crucial for the engine compatibility. In addition, hydrogen is a carbon-free clean fuel which is capable of relieving the environmental pollution.[1,2] Fundamental experiments of hydrogen combustion and accurate kinetic mechanisms that can represent the combustion characteristics of hydrogen are important to its application. Moreover, hydrogen combustion plays a prominent role in the combustion of hydrocarbon fuel as it contains many critical elementary reactions involving H, O, OH, H_2O, and HO_2, which serve as significant parts in all stages of the hydrocarbon combustion process.

Numerous H_2 kinetic mechanisms have been proposed in the literature.[3–13] For example, Hong *et al.*[3] proposed a H_2/O_2 mechanism based on reaction rate measurements. A hydrogen combustion mechanism was presented by Konnov *et al.*,[4] who paid particular attention to reaction HO_2+H, $OH+HO_2$, and to the pressure dependence of the recombination reaction of HO_2. Burke *et al.*[5] have developed an updated H_2/O_2 kinetic mechanism by incorporating recent improvements in rate constant and resolving discrepancies between experimental data and predictions based on Li *et al.*[6] A detailed kinetic mechanism has been built by Ó Conaire *et al.*,[7] which is applied to simulate the combustion of H_2/O_2 mixtures over a wide range of experimental conditions. This mechanism has been updated by Kéromnès *et al.*[8] for hydrogen and syngas mixtures with reaction rate constant expressions from both measurements and calculations. Recently, the updated mechanism has been optimized by Varga *et al.*[9] according to the sensitivity analysis carried out at each experimental data point. In the last four years, four hydrogen mechanisms have been proposed independently. The Curran group[10] built an AramcoMech 2.0 mechanism starting with a H_2/O_2 sub-mechanism that has been validated against a large array of experimental measurements, including data from shock tubes, rapid compression machines, flames, jet-stirred, and plug-flow reactors. The AramcoMech 2.0 mechanism has been widely used in the literature. The Ranzi group[11] at Politecnico di Milano proposed a detailed mechanism (CRECK) of hydrogen oxidation. The Ju group[12] from Princeton University built a comprehensive H_2/O_2 kinetic mechanism (HP-Mech) based on the combustion mechanism of Burke *et al.*[5] Another detailed combustion mechanism (San Diego) developed by Boivin *et al.*[13] was designed to focus on conditions relevant to flames, high temperatures

*Project supported by the National Key Research and Development Program of China (Grant Nos. 2017YFB0202400 and 2017YFB0202401).
†Corresponding author. E-mail: zhangchanghua@scu.edu.cn
© 2018 Chinese Physical Society and IOP Publishing Ltd

ignition, and detonations.

Though numerous hydrogen combustion kinetic mechanisms have been reported, few studies were involved in the comparison of various mechanisms. Comparisons among different experimental targets and mechanisms are often focusing on distinguishing the best performance mechanism. As reported in the literature,[14] the hydrogen mechanism of Keromnes *et al.*[8] yields the best agreement with data from ignition delay time at various pressures up to 16 atm, while the mechanisms of Davis *et al.*,[15] GRI 3.0,[16] San Diego-2011,[17] and Li *et al.*[6] present significantly poor predictions at higher pressures. Zamashchikov *et al.*[18] have investigated the laminar burning velocities of near-limit hydrogen flames and compared with three mechanisms[3–5] of hydrogen combustion. The discrepancy was found between experiments and mechanisms, indicating the need for further mechanism development.

Till now, various experimental measurements have been adopted to validate the kinetic mechanism for hydrogen combustion, including concentration time-profiles in a flow reactor and jet-stirred reactor, ignition delay time in a rapid compression machine and shock tube, and laminar flame velocity in a spherical bomb. Among these targets, species time-profiles can provide detailed verification on the reaction pathways and rate constants of reaction mechanisms used to simulate the chemistry of combustion processes. Thus, species concentration time-profiles are generally considered to be the favorite.[19] The laser absorption spectroscopy technique, due to its non-intrusive and fast time response, is suitable to monitor species time-histories accurately and directly.

In this paper, time-history data of H_2O during high-temperature oxidation of hydrogen were provided by laser absorption spectroscopy measurement in shock tube. A comparison between experimental results of H_2O time-histories and simulation results of hydrogen kinetic mechanisms was performed to validate the reliability of the mechanism.

2. Methodology

2.1. Shock tube setup

H_2O time-history experiments were carried out in a stainless steel shock tube with a 10 cm inner diameter. A double diaphragm section was used to separate the shock tube into a 2.0 m driver and a 5.0 m driven section. The experimental apparatus has been described in detail in the literature.[20,21] Polycarbonate diaphragms with a thickness of 0.05 mm were used to provide desired nominal reflected shock pressures. To eliminate the influence of the H-residual impurities and exhaust gas in the shock tube,[22] the whole driven section was flushed by high-purity argon, and the shock tube was evacuated to the pressure below 10^{-2} Torr by a vacuum pump system prior to each experiment, ensuring the accuracy of the measured data. Pure helium was used as the driven gas.

The incident shock velocity was obtained using four fast-response piezoelectric pressure transducers (PCB 113B, with rising time of less than 1.0 μs) mounted on the driven section of shock tube with the same length interval of 18.9 cm. The pressure time-histories were monitored using the last pressure transducer located at 15 mm from the end wall. The time intervals of shock passage were determined by the four pressure signals recorded by a digital phosphor oscilloscope (Tektronix TDS5054B). Three measured incident shock velocities were determined by linear extrapolation to obtain the shock velocity at the end wall. By using the one-dimensional normal shock relations, the reflected shock wave temperature (T) and pressure (P) behind the reflected shock wave can be obtained by the initial pressure and temperature measured in a driven section of the shock tube, the measured incident shock wave velocity at the endwall, and the composition and the thermodynamic properties of the $H_2/O_2/Ar$ mixtures. The 1.0 μs uncertainty in the velocity measurement will lead to 1.2% and 0.7% uncertainty in reaction pressure and temperature, respectively.

2.2. Laser absorption diagnostic technique

The schematic diagram of the tunable diode laser-absorption spectroscopy (TDLAS) experimental setup is shown in Fig. 1. A distributed feedback (DFB) mid-infrared diode laser around 2.55 μm from Nanoplus GmbH was used. The laser wavelength can be well controlled by a combination of injection current and temperature using a commercial controller (LCM 6000). The laser beam was collimated by a plano-convex lens and transmitted through the shock tube. A pair of flush mounted calcium fluoride windows providing optical access were located at 1.5 cm from the shock tube end wall, and the absorption path length is 10 cm. The transmitted laser was shielded by a narrow band-pass filter (center 2585 nm, half width: 500 nm) to avoid the radiation from the combustion process. Another plano-convex lens was used to reduce beam steering effects and focus the laser beam into an InGaAs detector (Thorlabs DET10D). The bandwidth of the detector is 14 MHz, which is sufficient for microsecond scale measurement. The signal was collected by a digital phosphor oscilloscope (Tektronix DPO5054). The whole beam path outside the shock tube was purged with pure nitrogen to minimize the laser attenuation due to ambient H_2O.

In this work, a fixed-wavelength direct-absorption strategy was employed in H_2O concentration time-history measurements. The DFB laser frequency was tuned to the peak of the v_3 fundamental vibrational band H_2O transition at 3920.09 cm^{-1}. This wavelength was selected primarily because of its favorable line strength and sufficiently isolated from adjacent lines.[23] Shortly before taking the data, the laser

was scanned over the water line to ensure that it was located at line center.[24,25] Typical operating conditions for the laser are 39.8 C and 57.02 mA.

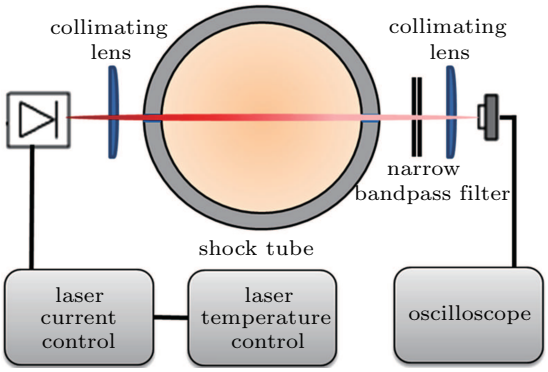


Fig. 1. Schematic diagram of the experimental setup.

H_2O time-history concentration was measured by tunable diode laser absorption spectroscopy using the Beer–Lambert law

$$I/I_0 = \exp(-X_{H_2O}\sigma P_i L), \tag{1}$$

where I_0 is the initial laser intensity, I is the transmitted laser intensity, X_{H_2O} is the H_2O mole fraction, L (cm) is the absorption path length of the sample, σ (m^2·mol^{-1}) is the absorption cross section of H_2O at the laser frequency, which is defined as

$$\sigma = S(T)\varphi(v)_{\max}, \tag{2}$$

where $\varphi(v)_{\max}$ is the maximum of the line-shape function and $S(T)$ (cm^{-2}·atm^{-1}) is the temperature-dependent line strength of the transition at temperature T (K). The $S(T)$ can be expressed in terms of the known line-strength at a reference temperature T_0 as

$$S(T) = S(T_0)\frac{Q(T_0)}{Q(T)}\exp\left[-\frac{hcE_i''}{k}\left(\frac{1}{T}-\frac{1}{T_0}\right)\right] \times \left[\frac{1-\exp(-hcv_0/kT)}{1-\exp(-hcv_0/kT_0)}\right], \tag{3}$$

where c (cm·s^{-1}) is the speed of light, v_0 (cm^{-1}) is the line center frequency, h (J·s) is Planck's constant, k (J·K^{-1}) is Boltzmann constant, $Q(T)$ is the partition function of the absorbing molecule, and E'' (cm^{-1}) is the lower state energy of the transition.

The line-shape function φ_v is given by the Voigt profile

$$\varphi(v) = \int_{+\infty}^{-\infty}\varphi_D(u)\varphi_C(v-u)\,\mathrm{d}u. \tag{4}$$

The Voigt profile can be characterized by the α parameter defined as

$$\alpha = \frac{\sqrt{\ln 2}\Delta v_C}{\Delta v_D}, \tag{5}$$

where Δv_C (cm^{-1}) is the full width at half maximum (FWHM) due to collisional broadening, Δv_C is the product of the sum of the mole fractions of each species and the system pressure at constant temperature. The total collision width in a multi-component environment can be expressed as

$$\Delta v_C = P\sum_i x_i 2\gamma_i. \tag{6}$$

The collisional broadening coefficient γ_i (cm^{-1}·atm^{-1}) can be calculated with the following scaling relation:

$$\gamma_i(T) = \gamma_I(T_0)(T_0/T)^n, \tag{7}$$

where n represents the temperature-dependent coefficient. The Δv_D (cm^{-1}) is the Doppler width, which can be calculated using

$$\Delta v_D = v_0\sqrt{\frac{8kT\ln 2}{mc^2}}. \tag{8}$$

In this study, the parameters such as $S(T_0)$, E'', and n were taken from the HITRAN database[26] for the water feature at 3920.09 cm^{-1}, the collisional broadening coefficient for argon $\gamma_{Ar} = 0.0277\times(296/T)^{0.50}$ (cm^{-1}·atm^{-1}) measured in shock tube experiments can be found in the literature.[23]

The temperature dependence of the cross-section σ at the measurement frequency (3920.09 cm^{-1}) for H_2O in argon at 2 atm is calculated by Eq. (2) and the results are shown in Fig. 2. The temperature dependence around 1100 K is relatively modest, which is advantageous in the present study of hydrogen oxidation. Uncertanties of 1.2% and 0.7% in reaction pressure and temperature lead to 0.5% uncertainly in H_2O concentration.

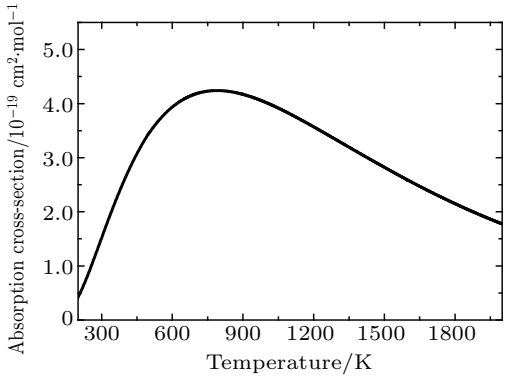


Fig. 2. Temperature dependence of the H_2O absorption cross-section at 3920.09 cm^{-1} for H_2O.

2.3. Mixture preparation

Test gas mixtures were prepared manometrically in a 40 liter stainless steel mixing tank by Dalton's law of partial pressure. The hydrogen was aerated into the vacuum tank, and diluted by oxygen and argon. The pressures of hydrogen and oxygen were monitored through a capacitance manometer of

the tank, and argon gas pressure was measured by a pressure gauge. Two mixtures with highly diluted argon were studied in this work: $X_{H_2} = 1\%$, $X_{O_2} = 1\%$, $X_{Ar} = 98\%$, and $X_{H_2} = 0.5\%$, $X_{O_2} = 1\%$, $X_{Ar} = 98.5\%$. The reflected shock pressure was 2 atm and the temperatures were 1110–1282 K. The dilution is sufficient so that the temperature rise due to heat release throughout the time duration can be ignored.

2.4. Kinetic mechanism simulation

One objective of the current work is to use our measured H_2O time-histories during oxidation of hydrogen to evaluate the performance of kinetic mechanisms. In this study, four major independent mechanisms published since 2014 are considered and the details of these mechanisms are provided in Table 1. Simulations of H_2O time-histories were performed using the Chemkin software.[27] A constant-volume (constant U, V) and constant-internal-energy modeling constraint was applied under reflected shock wave conditions in this study.

Table 1. Details of the hydrogen kinetic mechanism investigated in this study.

No.	Mechanism	Ref.	Update date	Species	Reactions
1	AramcoMech 2.0	[10]	2016	12	34
2	CRECK	[11]	2014	11	20
3	HP-Mech	[12]	2017	11	26
4	San Diego	[13]	2016	11	23

3. Results and discussion

Figure 3 shows a typical single-shot measurement result, including reflected shock pressure, mid-infrared diode laser signal, and the H_2O time-histories. The time-history of the H_2O concentration was calculated from Eqs. (1)–(8) based on measured laser signal I/I_0. In Fig. 3(b), the laser signal before the arrival of the incident shock is I_0. The typical data were obtained in a 1% H_2/1% O_2/Ar mixture at initial conditions of 1246 K and 2 atm. Two sharp rises in the pressure trace are the arrival of the incident and reflected shock wave. The reflected pressure is relatively flat in 1.2 ms. Time zero is set as the arrival of the reflected shock wave. The pressure fluctuation is less than $\pm 1.5\%$, and the estimated temperature increase is less than 0.8%. The laser transmission histories signal shows two sharp Schlieren spikes[28] around time zero, which coincide with the passage of the incident and reflected shock waves. These two sharp peaks are caused by the deflection of the laser beam on the density gradients of a shock wave front zone. In this work, we define the first-stage ignition delay as the time spacing between the extrapolation of the steepest rise in measured H_2O concentration and the arrival of reflected shock waves at the endwall, as shown in Fig. 3(c). After a first-stage ignition delay of 280 μs where chain carrier radials (H, O, and OH) were being accumulated, the H_2O concentration increased gradually. At about 400 μs, the H_2O concentration reaches its maximum, indicating the termination of the combustion reaction.

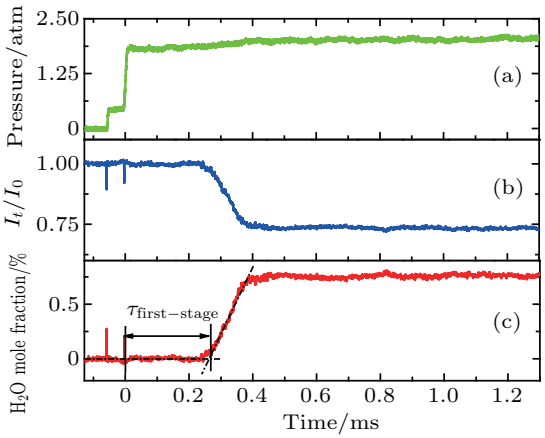


Fig. 3. (a) Typical reflected shock pressure, (b) laser transmission signal, and (c) the time dependence of the H_2O mole fraction for 1% H_2/1% O_2/98% Ar mixture. $T = 1246$ K, $P = 2$ atm.

A systematic measurement related to the H_2O time-histories was performed behind the reflected shock wave at different temperatures and equivalences. As shown in Fig. 4, the combustion kinetic mechanisms were evaluated by the experimental data. At an equivalence ratio of 0.5 and temperature at 1170 K (Fig. 4(a)), the first-stage ignition delay time of CRECK fits well with the measurement data, but this mechanism over-predicts the H_2O time-history formation profile. By contrast, the San Diego, AramcoMech 2.0, and HP-Mech mechanisms over-predict the first-stage ignition delay time, while the H_2O time-history formation profiles of San Diego and AramcoMech 2.0 mechanism fit well with the experimental data. At an equivalence ratio of 0.5 and temperature at 1246 K (Fig. 4(b)), and at an equivalence ratio of 0.25 (Fig. 4(c) and Fig. 4(d)), the CRECK mechanism under-predicts the first-stage ignition delay time and over-predicts the H_2O time-history formation profile. The HP-Mech over-predicts the first-stage ignition delay time and under-predicts the H_2O time-history formation profile. The simulation results of San Diego and AramcoMech 2.0 mechanisms fit well with the first-stage ignition delay time and the H_2O time-history of the experiment, with AramcoMech 2.0 being more consistent.

According to the comparison between the measured data with the simulation results of mechanisms under all experimental conditions, the performance of CRECK, HP-Mech, and San Diego mechanisms is unsatisfactory, while the AramcoMech 2.0 mechanism performs best. The simulation discrepancy between these four mechanisms may come from the difference in the reaction pathways, which is determined by the rate constants of the important reactions. Pathways analysis is carried out to further explain the discrepancy.

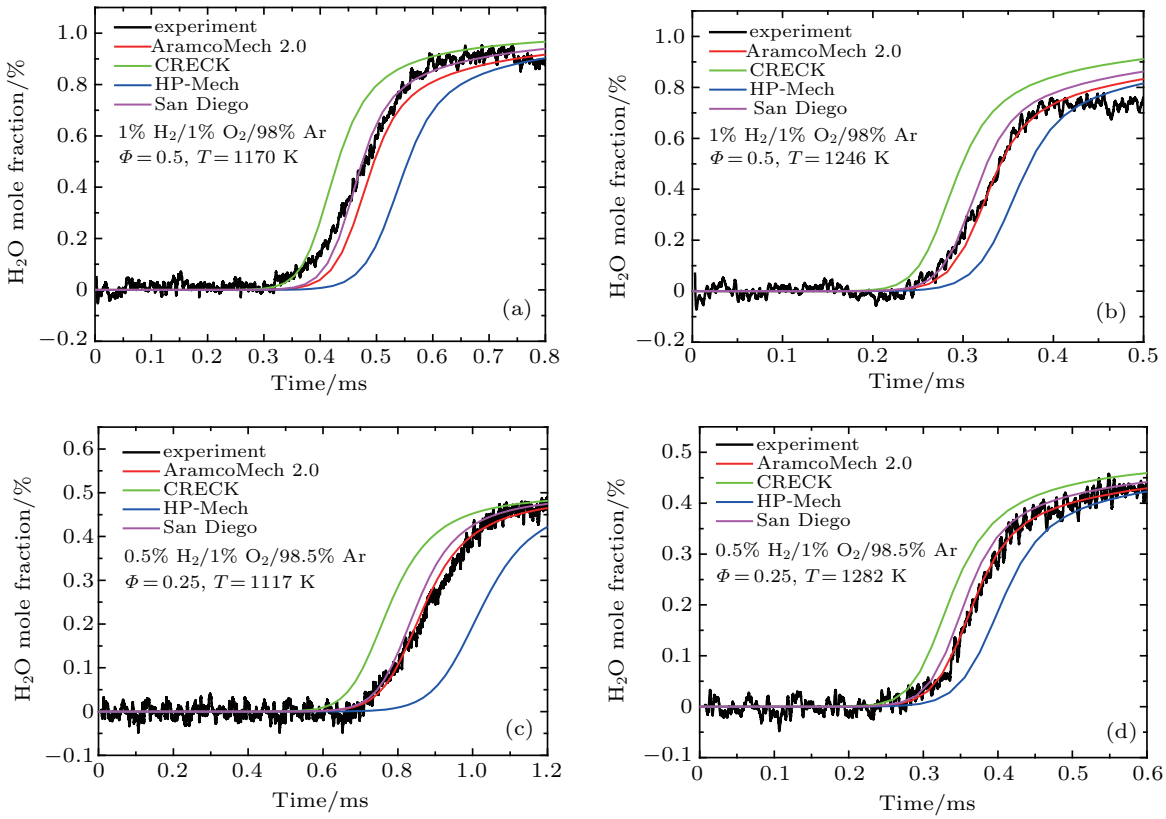


Fig. 4. Measured and calculated H_2O time-histories at different conditions.

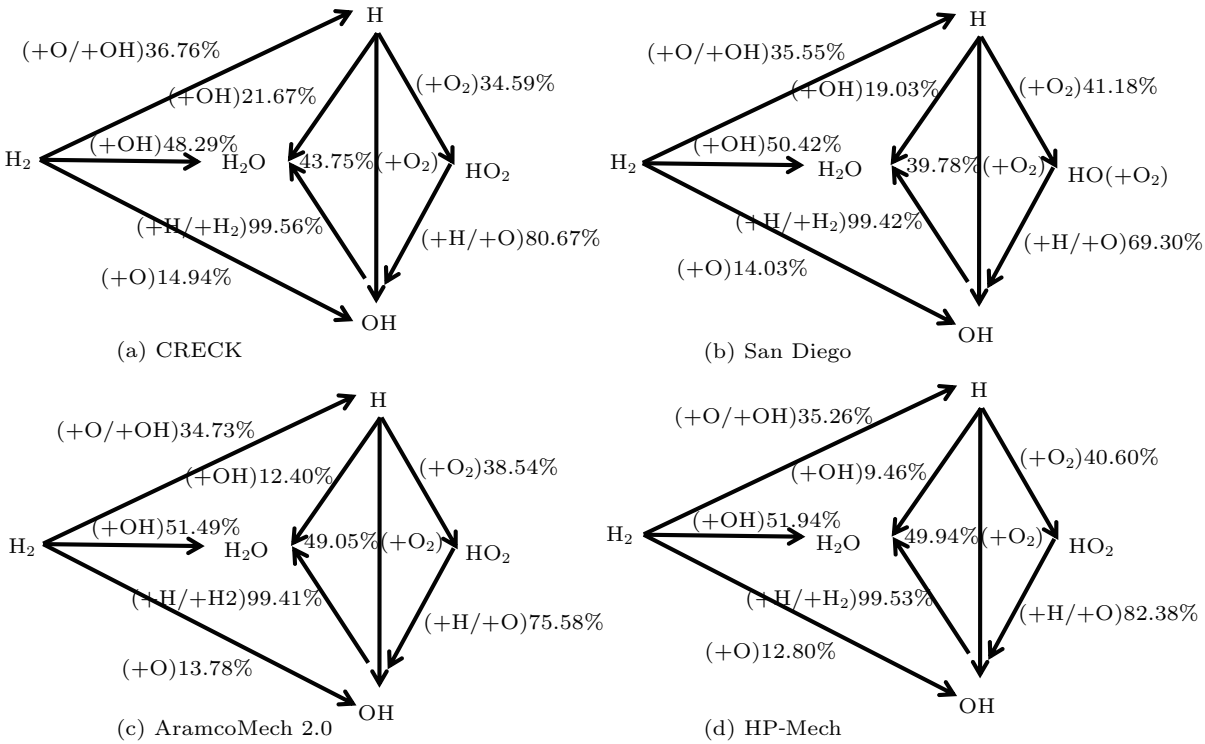


Fig. 5. Time-integrated element flux analysis of hydrogen at $T = 1170$ K, $P = 2$ atm, and $\Phi = 0.5$. The values are the conversion percentages of H.

To understand the combustion controlling the H_2O formation during the combustion of hydrogen, reaction pathway analysis was carried out to investigate the important reaction pathways of H_2O formation. A time-integrated H element flux analysis method[29] was employed to analyze the reaction pathway. An in-house package is developed and coupled with CHEMKIN libraries to post-process the results of kinetic simulations. Reaction pathway analysis of the four mechanisms was conducted at $T = 1170$ K, $P = 2$ atm, and $\Phi = 0.5$ to confirm the controlling steps. The percentage of the con-

versions is defined as the percentage of the flux of element H atom from one species to another with respect to the total flux of H. As shown in Fig. 5, H-abstraction by O and OH radicals is the dominated pathway consuming hydrogen by two reactions: $H_2+O=H+OH$ and $OH+H_2=H+H_2O$, subsequently, the generated H radicals are primarily consumed by three paths: $H+O_2=O+OH$, $H+OH+M=H_2O+M$, and $H+O_2(+M)=HO_2(+M)$. The major difference of these pathways in these mechanisms is the conversion rate from H to H_2O by the reaction $H+OH+M=H_2O+M$. In CRECK, the conversion rate is 21.67%, while in San Diego it is 19.03%. This value decreases to 12.40% and 9.46% in AramcoMech 2.0 and the HP-Mech mechanism, respectively. As the conversion rate of reaction $H+OH+M=H_2O+M$ decreases, the predicted H_2O time-history formation profile decreases and first-stage ignition delay increases. The CRECK mechanism that over-predicts the measured H_2O time-history formation profiles has a higher conversion rate, while the HP-Mech mechanism which under-predicts the measure H_2O time-history formation profiles has a lower reaction conversion rate. Based on the above discussion, we can conclude that the different conversion rate of the reaction $H+OH+M=H_2O+M$ among these mechanisms induces the different prediction result.

4. Conclusions

Time-histories measurements of H_2O are investigated during the highly dilute oxidation of hydrogen in reflected shock tube experiment carried out at the temperature 1170–1282 K, the equivalence ratios of 0.5 and 0.25, and pressure around 2 atm. A fixed-wavelength strategy was applied to measure the H_2O time-history using tunable diode laser-absorption spectroscopy in the mid-infrared near 2.55 μm. Measured time-histories of H_2O were evaluated with four independent hydrogen reaction mechanisms agreed in the last four years. The performances of CRECK, HP-Mech, and San Diego mechanisms are unsatisfactory, while only the AramcoMech 2.0 mechanism agrees well with the experimental data in the investigated conditions. Further reaction pathway analysis indicates that the reaction $H+OH+M=H_2O+M$ is the key reaction in controlling the H_2O formation during the oxidation of hydrogen. It is inferred that different performance on H_2O time-history predictions among these four mechanisms is due to the discrepancy of the reaction pathways, which is determined by the rate constants of the important reactions. Current results confirm the feasibility of H_2O time-history measurements for future development of combustion kinetic mechanisms.

References

[1] Tang C L, Zhang Y J and Huang Z H 2014 *Renew. Sust. Energ. Rev.* **30** 195
[2] Jain I P 2009 *Int. J. Hydrogen Energy* **34** 7368
[3] Hong Z K, Davidson D F and Hanson R K 2011 *Combust. Flame* **158** 633
[4] Konnov A A 2008 *Combust. Flame* **152** 507
[5] Burke M, Chaos M, Ju Y G, Dryer F L and Klippenstein S J 2012 *Int. J. Chem. Kinet.* **44** 444
[6] Li J, Zhao Z W, Kazakov A and Dryer F L 2004 *Int. J. Chem. Kinet.* **36** 566
[7] Ó Conaire M, Curran H J, Simmie J M, Pitz W J and Westbrook C K 2004 *Int. J. Chem. Kinet.* **36** 603
[8] Kéromnès A, Metcalfe W K, Heufer K A, Donohoe N, Das A K, Sung C J, Herzler J, Naumann C, Griebel P, Mathieu O, Krejci M C, Petersen E L, Pitz W J and Curran H J 2013 *Combust. Flame* **160** 995
[9] Varga T, Nagy T, Olm C, Zsély I G, Pálvölgyi R, Valko E, Vincze G, Cserháti M, Curran H J and Turányi T 2015 *Proc. Combust. Inst.* **35** 589
[10] Zhou C W, Li Y, O'Connor E, *et al.* 2016 *Combust. Flame* **167** 353
[11] Ranzi E, Frassoldati A, Grana R, Cuoci A, Faravelli T, Kelley A P and Law C K 2012 *Prog. Energy Combust. Sci.* **38** 468
[12] Zhao H, Fu J P, Haas F M and Ju Y G 1991 *Combust. Flame* **183** 253
[13] Boivin P, Sánchez A L and Williams F A 2017 *Combust. Flame* **176** 489
[14] Hu E J, Pan L, Gao Z H, Lu X, Meng X and Huang Z H 2016 *Int. J. Hydrogen Energy* **41** 13261
[15] Davis S G, Joshi A V, Wang H and Egolfopoulos F 2005 *Proc. Combust. Inst.* **30** 1283
[16] Smith G P, Golden D M, Frenklach M, Moriarty N W, Eiteneer B, Goldenberg M, Bowman C T, Hanson R K, Song S, Gardiner W C, Lissianski V V and Qin Z http://www.me.berkeley.edu/gri_mech [2010]
[17] Niemann U, Seshadri K and Williams F A 2013 *Proc. Combust. Inst.* **34** 881
[18] Zamashchikov V V, AlekseevV A and Konnov A A 2014 *Int. J. Hydrogen Energy* **39** 1874
[19] Hanson R K and Davidson D F 2014 *Prog. Energy Combust. Sci.* **44** 103
[20] Zhang C, He J, Li Y, Li X and Li P 2015 *Fuel* **154** 346
[21] Zhang C H, Li P, Guo J J and Li X Y 2012 *Energy Fuels* **26** 1107
[22] Urzay J, Kseib N, Davidson D F, Iaccarino G and Hanson R K 2014 *Combust. Flame* **161** 1
[23] Hong Z K, Farooq A, Barbour E A, Davidson D F and Hanson R K 2009 *J. Phys. Chem. A* **113** 12919
[24] Gou Y D, Lu P F, He J N, Zhang C H, Li P and Li X Y 2018 *Spectrosc. Spect. Anal.* **38** 176 (in Chinese)
[25] Xia H H, Kan R F, Liu J G, Xu Z Y and He Y B 2016 *Chin. Phys. B* **25** 064205
[26] Rothman L S, Gordon I E, Babikov Y, *et al.* 2013 *J. Quant. Spectrosc. Ra.* **130** 4
[27] ANSYS CHEMKIN 17.0 (15151), ANSYS Reaction Design: San Diego 2016
[28] Tekawade A, Kosiba G and Oehlschlaeger M A 2016 *Combust. Flame* **173** 402
[29] Wang Q D, Fang Y M, Wang F and Li X Y 2013 *Proc. Combust. Inst.* **34** 187